An Automatic 3D Work Object Calibration Method Based on Hybrid 2D Image Vision

C. K. Huang, C. Y. Yang, B. C. Hsu, Yi-Ying Lin, and C. H. Chen
Intelligent Machinery Technology Center, Industrial Technology Research Institute, Hsinchu, Taiwan
Email: itriA50317@itri.org.tw

***Abstract*—The coordinates of the tool center point (TCP) relative to work object coordinate frame of a robotic arm or manipulator indicates the action of the arm. Therefore, the absolute accuracy of the manipulator is subject to the precision of the TCP relative to the work object coordinate system. Improving the precision of the manipulator's motion requires calibrating the TCP and work object coordinate frame respectively. An work object coordinate frame automatic calibration of the manipulator's work object coordinate frame typically involves installing image sensors and calibrating the installing position or control the tool to touch the work object for it, whereas a manual calibration procedure, whose precision depends on the operator's experience and technical competence. To address the limitations in existing work object coordinate frame calibration procedures, this paper presents an automatic calibration method that involves using an image sensors with hybrid 2D image vision, and performing visual servo control to calibrate the TCP. The presented method can efficiently calibrate the work object frame in 1 min.**

***Index Terms*—work object coordinate frame, automatic calibration, industrial robot, visual servo**

I. Introduction

With the development of automatic production, robotic arms have been widely applied in industry. According to the predictions of the International Federation of Robotics, 3.971 million robotic arms will be in operation by 2022[1]. These arms greatly improve the efficiency and quality of industrial production. In the technical field of robotic-arm-based automation, tools are generally installed on the robotic arms, and arm movements are driven by orders manually teach by users to achieve automatic applications. However, because of the increasing complications associated with robotic arm trajectories and the development of offline programing, the accuracy of the path is influenced by the path of the robotic arms; additionally, the precision of the relative relationship between the work object coordinate frame (WOCF) and robotic arms directly affects the precision of robotic arm movements. Therefore, the accuracy of the WOCF is an essential indicator of precise robotic arm operation.

The automation of robotic arms requires advance verification of the positional relationship between the work object and robotic arms; however, the positioning of a work object is not a simple operation, and deviations of the WOCF may occur because of an imprecise positioning device or dimensional tolerances. Hence, work object positions should be calibrated so that accurate coordinates are obtained prior to a robotic arm operation. Conventional calibration of work object position is conducted through manual orders. The tool center point (TCP) is adjusted to coincide with several designated points on the work object, and the coordinates are marked down to complete the work object calibration. The present automatic calibration approach has the following disadvantages. (1) The TCP need to contact with the work object, which is likely to result in damage to the work object and deviations caused by personnel operation [2][3]. (2) A sensor is installed on the exterior, and the work object coordinates are adjusted through coincidence of the designated point or measurement of the actual distance to the target point; because various tools can be employed, the designated point may be obscured by the object itself or the tool and thus cannot be observed [4][5]. (3) The distance between the robotic arm and calibration instrument or work object is measured using a CAD model, but this type of measurement is time consuming, and feature points on the work object are required to reduce deviation in the measurement [6][7].

Given the aforementioned obstacles, this paper proposes an automatic work object coordinate frame calibration method. An image sensor is installed on the robot flange (the first visual sensor); a second visual sensor is established using a multiple-view approach; and the first and second visual sensors are combined to generate a 2.5D image. Subsequently, an arbitrary point within the intersection of the first and second visual sensors is selected as a virtual TCP, and this point is made to coincide with the virtual TCP of the visual servo controlled robotic arm as well as the designated point of the WOCF. The calibration of the WOCF is completed using a relatively simple operation sequence in which the problems of the current measure are solved (saving the expense of manual labor and time and avoiding damage to the work object) and the calibration accuracy is improved.

II. Automatic Work Object Calibration Techniques

In practice, tools are attached to the flange (end effector) of robotic arms, and during the operation of the tools, the coordinate systems of the TCP and work object should be

Manuscript received September 4, 2019; revised May 21, 2020.

doi: 10.18178/joace.8.1.20-25

defined to describe the actions of the robotic arms according to the relationship between the two coordinate frames. However, deviations may occur in work object positioning due to the methods of securing the work object, precision of the positioning mechanism, or dimensional tolerance of the work object; Therefore, calibration is required if coordinates are to be accurate. The paper proposes a visual calibration method concerning work object position and for obtaining the WOCF. This automatic work object calibration method is explained in this section.

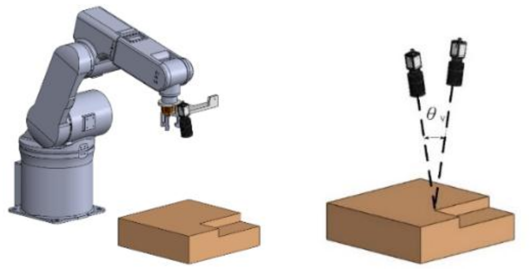

(a) Automatic work object calibration (b) Hybrid vison

Figure 1. Automatic work object calibration system

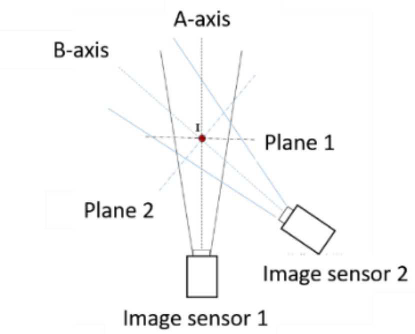

Figure 2. Construction of 2.5D vision using the hybrid 2D images

A robotic arm, work object, and image sensors installed on the robot flange are employed in this method (Fig. 1). A multiple-view approach (image sensors 1 and 2 project the first and second visual sensors, respectively) is used to obtain 2.5D vison. The axes of image sensors 1 and 2 are defined as the A-axis and B-axis; planes 1 and 2 pass through the intersection of the two axes and are perpendicular to the A-axis and B-axis, respectively (Fig. 2). I_1 and I_2 are the coordinates of two points within the intersection of the two views generated by the image sensors, and the intersection point of the two image sensor axes is the virtual TCP (Point I).

The calibration procedure is divided into four parts: (1) installation of the image sensors on the robot flanges; (2) establishment of a transformation relationship between the coordination frames of the robot flange and image sensor to convert the action gathered by the sensor into action of the robotic arm; (3) construction of the second visual sensor, location of the virtual TCP with a hybrid vision approach to generate 2.5D machine vision, and determination of the coordinates of the virtual TCP (I); and (4) control of the robotic arm by using the visual servo, so that point I coincides with the designated points on the work object. Finally, the actual work object coordinates are calculated. Each part of the procedure is specified in the following sections.

A. Establishment of the Transformation Relation between the Robot Flange and Image Sensor Coordinate Frames

The transformation relation between the robotic arm and image sensor reference coordinate frames is established as follows: the tool center is moved along the three axes of the robotic arm reference coordinate frame $x_R - y_R - z_R$; the plane vector (x_i, y_i) of the image sensor coordinate frame $x_c - y_c - z_c$ corresponding to the three axes during the movement is retrieved, and the transformation relation between the two reference coordinate frames is obtained on the basis of the perpendicularity of the vectors, as illustrated in Fig. 3. The procedure is as follows:

1. The robotic arm is moved to an arbitrary position within the vision of the image sensor, and this point is defined as the origin point (referred to as O in the following section) of the image sensor coordinate frame.
2. Point O is moved along the x_R direction of the robotic arm coordinate frame for an arbitrary length to obtain the projection point $\mathrm{P}'_x = (x_1, y_1, 0)$ of the image sensor, and the space vector of the point is defined as $\mathbf{U_1} = (-x_1, -y_1, -z_1)$.
3. Point O is moved along the y_R direction of the robotic arm coordinate frame for an arbitrary length to find the projection point $\mathrm{P}'_y = (x_2, y_2, 0)$ of the image sensor, and the space vector of the point is defined as $\mathbf{V_1} = (-x_2, -y_2, -z_2)$.
4. Point O is moved along the z_R direction of the robotic arm coordinate frame for an arbitrary length to determine the projection point $\mathrm{P}'_z = (x_3, y_3, 0)$ of the image sensor, and the space vector of the point is defined as $\mathbf{W_1} = (-x_3, -y_3, -z_3)$.
5. Based on the perpendicularity of the coordinate frame, the simultaneous equations $\mathbf{U_1} \cdot \mathbf{V_1} = 0, \mathbf{V_1} \cdot \mathbf{W_1} = 0, \mathbf{U_1} \cdot \mathbf{W_1} = 0$ are obtained with constant vectors $\mathbf{U_1}, \mathbf{V_1}$, and $\mathbf{W_1}$. The first and second solutions of the equations are $(\mathrm{z}_{11}, \mathrm{z}_{21}, \mathrm{z}_{31})$ and $(\mathrm{z}_{12}, \mathrm{z}_{22}, \mathrm{z}_{32})$, and the difference between them is $(\mathrm{z}_{11}, \mathrm{z}_{21}, \mathrm{z}_{31}) = -(\mathrm{z}_{12}, \mathrm{z}_{22}, \mathrm{z}_{32})$. Therefore, the variation in the distance between two arbitrary feature points on the work object can be used to determine whether the fixed point moves toward or away from the image sensor when it moves in the direction of the robotic arm base reference coordinate frame $x_R - y_R - z_R$, and the accurate branch solution can be calculated.
6. The coordinate of the image sensor in the robot flange reference coordinate frame is ${}^{\mathrm{flange}}\mathrm{T}_{\mathrm{CCD}} = \left({}^{\mathrm{base}}\mathrm{T}_{\mathrm{flange}}\right)^{-1} \left[\frac{\mathbf{U_1}}{\|\mathbf{U_1}\|} \; \frac{\mathbf{V_1}}{\|\mathbf{V_1}\|} \; \frac{\mathbf{W_1}}{\|\mathbf{W_1}\|}\right]^{-1}$, with ${}^{\mathrm{flange}}\mathrm{T}_{\mathrm{CCD}}$ being the coordinate of the image sensor in the robot flange reference coordinate frame and ${}^{\mathrm{base}}\mathrm{T}_{\mathrm{flange}}$ being the coordinate of the robot flange relative to the base reference frame.

7. The obtained relation between the robotic arm and image sensor reference coordinate frames is $\boldsymbol{S_R} = {}^{\text{base}}\text{T}_{\text{flange}}\,{}^{\text{flange}}\text{T}_{\text{CCD}}\boldsymbol{S_c}$, with $\boldsymbol{S_c}$ being the amount of movement along the image sensor coordinate frame $x_c - y_c - z_c$, and S_R the amount of movement along the robotic arm reference coordinate frame $x_R - y_R - z_R$.

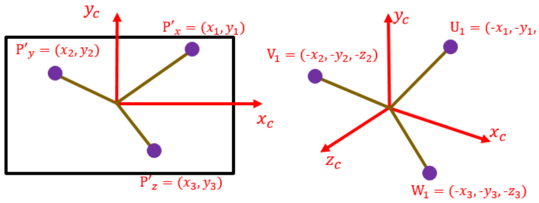

Figure 3. Transformation relation between the coordinate frames

B. Construction of the Second Visual Image Sensor

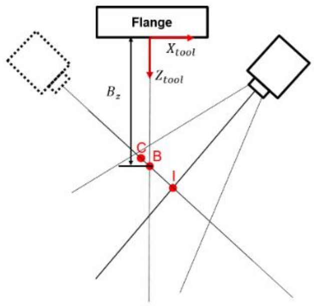

Figure 4. Transformation relation between the coordinate frames

Once the transformation relation between the robot flange and image sensor coordinate frames has been established, the image sensor is rotated around a point within the visual field (referred to as the virtual TCP in the following sections) regarding an arbitrary axis of the robot flange at an angle of θ_v to construct a second visual, and the current location of the sensor is defined as image sensor 2. The method of obtaining the virtual TCP and constructing a second visual sensor is as follows:

1. The robotic arm is moved to an arbitrary feature point C within the visual field, and the coordinate of another arbitrary feature point B within the visual field is defined as $\mathbf{B} = [B_x \quad B_y \quad B_z]$ concerning the robot flange, as illustrated in Fig. 4. The coordinates of point **B** are estimated values that can be obtained through on-site measurement or using a CAD model.
2. The coordinates of **C** in the image coordinate frame (C_1) with image sensor 1 are obtained, and the sensor is rotated around the z_c-axis at two angles to generate coordinates $\mathbf{C_2}$ and $\mathbf{C_3}$. The circular arc formed by $\mathbf{C_1}$, $\mathbf{C_2}$, and $\mathbf{C_3}$ is used to calculate the location of the circle center B_1, as illustrated in Fig. 5.
3. The vector $(\mathbf{B_1I_1})_c$ of B_1 to the center point in the visual field is calculated, and the vector $(\mathbf{B_1I_1})_c$ relative to the image sensor coordinate frame is converted into $(\mathbf{B_1}\boldsymbol{I_1})_f = {}^{\text{flange}}\text{T}_{\text{CCD}}(\mathbf{B_1I_1})_c$ with respect to the robot flange.
4. The coordinates of point B are corrected into $\mathbf{B} = \mathbf{B} + \mathbf{L}(\mathbf{B_1}\boldsymbol{I_1})_f$, with L being an arbitrary constant. The procedure is then repeated from step 1 until point B_1 coincides with I, and the coordinate I of the virtual TCP is thus found.
5. The image sensor is rotated around an arbitrary axis of the robot flange at an angle of θ_v to obtain a second visual sensor, and the current location of the sensor is defined as image sensor 2.

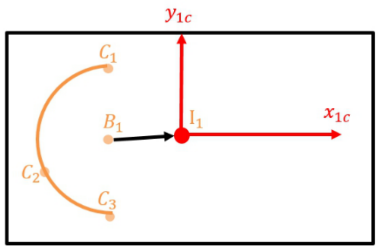

Figure 5. Image sensor centre point approaching in the second visual

C. Obtaining the Designated Point on the Work Object

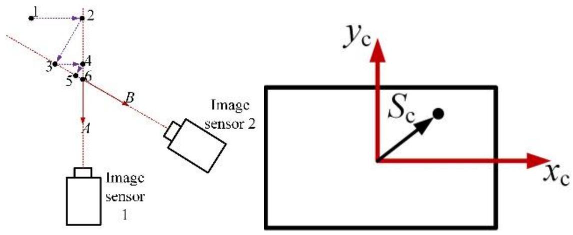

Figure 6. Direction of movement concerning the two reference coordinate frames

In terms of calculation of the WOCF, the paper explains the method for obtaining the designated point by using the origin point, an arbitrary point on the X-axis, and an arbitrary point on X-Y plane. The method can be employed to calculate the position of the WOCF and obtain the coordinates of the designated point. The procedures are as follows:

1. The robotic arm is moved to include the first designated point in the visual field of the image sensor, the point is defined as the origin in the image coordinate frames of image sensors 1 and 2, and i = 1.
2. The data collected from image sensor 1 are processed with visual servo control, and the designated point is made to coincide with the origin point in the image sensor 1 coordinate frame.
3. The data gathered from image sensor 2 are processed with visual servo control, and the designated point is made to coincide with the origin point in the image sensor 2 coordinate frame.
4. Steps 2 and 3 are repeated to make the designated point approach the virtual TCP until the deviation between the virtual TCP and designated point is smaller than the permissible value, as depicted in Fig. 6.
5. Let $\text{i} = \text{i} + 1$. If $\text{i} \leq$ the number of designated points, the process is returned to step 2. The robotic arm is moved to make the number i designated point within the intersection of the two visual

sensors. If i > the number of designated points, the designated point data-gathering process is complete.

D. Moving the Visual Servo Controlled Robotic Arm to the Axes' Intersection

Regarding how the work object is moved on the axes by using visual servo control, the coordinates of the designated point in the image sensor coordinate frame can be obtained from the image captured by the image sensor, and the control can be completed after the direction of movement has been calculated. The explanation is as follows:

1. The coordinates (x_{c1}, y_{c1}) of the designated point relative to the image sensor are obtained using data collected by the image sensor.
2. The direction of movement $\boldsymbol{S_c} = \frac{(x_{c1}, y_{c1})}{\sqrt{{x_{c1}}^2 + {y_{c1}}^2}}$ is converted into the direction of the robotic arm coordinate frame $\boldsymbol{S_R} = {}^{\text{base}}\text{T}_{\text{flange}}\, {}^{\text{flange}}\text{T}_{\text{CCD}} \boldsymbol{S_c}$, as depicted in Fig. 6.
3. The robotic arm is moved in that direction until the designated point reaches the axes in the image sensor coordinate frame.
4. If the designated point is not on the center point of the visual field, the process returns to step 1. If the designated point coincides with the axes' intersection, the visual servo control process is complete.

E. Calculation of the Actual Position of the WOCF

The position of the WOCF is calculated according to the frame's origin point $\mathbf{W_o}$, a point $\mathbf{W_x}$ on the X-axis, and a point $\mathbf{W_{x-y}}$ on the X-Y plane:

1. Equation for calculating the X-axis direction: $\widehat{e_x} = \frac{\mathbf{W_x} - \mathbf{W_o}}{\|\mathbf{W_x} - \mathbf{W_o}\|}$
2. Equation for calculating the Z-axis direction: $$\widehat{e_z} = \widehat{e_x} \times \frac{\mathbf{W_{x-y}} - \mathbf{W_o}}{\|\mathbf{W_{x-y}} - \mathbf{W_o}\|} \Bigg/ \left\| \widehat{e_x} \times \frac{\mathbf{W_{x-y}} - \mathbf{W_o}}{\|\mathbf{W_{x-y}} - \mathbf{W_o}\|} \right\|$$
3. Equation for calculating the Y-axis direction: $\boldsymbol{\widehat{e_y}} = \boldsymbol{\widehat{e_z}} \times \boldsymbol{\widehat{e_x}}$
4. The transformation matrix of the WOCF relative to the robotic arm base coordinate frame: WORK = $\begin{bmatrix} \boldsymbol{\widehat{e_x}} & \boldsymbol{\widehat{e_y}} & \boldsymbol{\widehat{e_z}} & \mathbf{W_o} \\ 0 & 0 & 0 & 1 \end{bmatrix}$

III. Testing the WOCF Calibration System

To verify the theory presented in Section 2, the proposed method establishes the robotic arm automatic WOCF calibration system and incorporates the 7A6 robotic arm designed by Industrial Technology Research Institute. The calibration system is as shown in Fig. 7, and the D-H parameters are listed in Table I (unit of length: mm). The system is mainly composed of a 2D image sensor installed on the robotic arm end effector and a control unit.

Figure 7. Work object coordinate frame calibration system

TABLE I. D-H Link Parameters of the 7A6 Robotic Arm

D-H link parameters	$\boldsymbol{a_i}$	$\boldsymbol{d_i}$	$\boldsymbol{\alpha_i}$	$\boldsymbol{\theta_{imin}}$	$\boldsymbol{\theta_{imax}}$
1	80	350	−90°	−170°	170°
2	270	0	0°	−60°	135°
3	100	0	−90°	−40°	170°
4	0	350	90°	−180°	180°
5	0	0	−90°	−100°	100°
6	0	100	0°	−360°	360°

The work object is placed randomly within the movement range of the robotic arm, and an arbitrary feature point is then selected using the image sensor (a cusp in the space is defined as the feature point in the proposed method). Subsequently, in the image sensor coordinate frame, the motion vectors of the designated point are identified by moving the arm along the $x_R, y_R,$ and z_R axes separately. The processing of the images obtained by the image sensor is divided into two parts: preprocessing and main processing. During preprocessing, the morphology of the work object is acquired by employing a Canny edge detector, and grayscale is eliminated using the binarization process. Subsequently, noise is removed using opening and closing operations according to the mathematical morphology proposed by Matheron and Serra. For the main processing, morphology data were searched for on the basis of the Hough transform, and the distance transform was employed to determine the coordinates of the feature point. When the image sensor vectors of $x_R, y_R,$ and z_R have been obtained, the transformation relation between the image sensor and robotic arm coordinate frames can be acquired using the method introduced in Section 2A, and Equations (1) and (2). Once the transformation matrix of image sensor 1 has been calculated, the three-dimensional coordinates of an arbitrary point within the visual field are estimated, and the point is then set as the rotation point. By using the method explained in Section 2B and rotating image sensor 1 around the Z-axis by 180° to construct the second image sensor (image sensor 2), the system is established. Equation (3) is the transformation matrix of image sensor 2.

$$\mathbf{U_1} = \begin{bmatrix} 326 \\ -2 \\ -95.54 \end{bmatrix}, \mathbf{V_1} = \begin{bmatrix} 2 \\ 410 \\ -1.7585 \end{bmatrix}, \mathbf{W_1} = \begin{bmatrix} 205 \\ 2 \\ 699.4726 \end{bmatrix} \quad (1)$$

$$^{\mathbf{flange}}\mathbf{T_{CCD1}} = \begin{bmatrix} 0.9596 & 0.0049 & 0.2812 \\ -0.0059 & 1 & 0.0027 \\ -0.2812 & -0.0043 & 0.9596 \end{bmatrix} \quad (2)$$

$$^{\mathbf{flange}}\mathbf{T_{CCD2}} = \begin{bmatrix} -0.9596 & -0.0049 & 0.2812 \\ 0.0059 & -1 & 0.0027 \\ 0.2812 & 0.0043 & 0.9596 \end{bmatrix} \quad (3)$$

where $\mathbf{U_1}, \mathbf{V_1}$, and $\mathbf{W_1}$ are the vectors of image sensor 1, whereas $^{\mathrm{flange}}\mathrm{T_{CCD1}}$ and $^{\mathrm{flange}}\mathrm{T_{CCD2}}$ are the transformation matrices of image sensors 1 and 2, respectively.

TABLE II. CALIBRATION REFERENCE POINTS

	x (mm)	*y (mm)*	*z (mm)*
Virtual TCP	***50.124***	***2.641***	***110.657***
Work object origin point	***497.105***	***65.800***	***88.004***
Work object X-axis	***603.007***	***-19.529***	***88.007***
Work object X-Y plane	***562.763***	***-158.232***	***88.007***

After the preceding procedures have been completed, the transformation matrix of WOCF can be obtained using the method presented in Section 2.5 as follows:

$$\mathrm{WORK} = \begin{bmatrix} 0.7787 & -0.6274 & 0 & 497.105 \\ -0.6274 & -0.7787 & 0 & 65.8 \\ 0 & 0 & -1 & 88.004 \\ 0 & 0 & 0 & 1 \end{bmatrix} \quad (4)$$

Based on the aforementioned examples, the TCP of a robotic arm can be quickly and automatically calculated using the method proposed by the present study. Therefore, this method can be applied to tool change calibration, tool wear compensation in long-term use, and self-examination on accuracy when using robotic arms.

IV. CONCLUSION

The current development of domestic automation intelligence applications is mostly reliant on models designed by international corporations, including the Japanese FANUC, Mujin, and Keyence, which have 80% of the market share. Accordingly, the price, delivery time, and profit of the domestic automation intelligence applications are subjected to other countries. Advanced automatic application techniques are not easy to develop and require extensive input in development and output in application achievements. Industry owners in Taiwan have expressed considerable faith in the open structure and functions of domestic-made controllers, increasing the willingness of end users to switch from Japanese- or European-made controllers to domestic-made controllers with higher cost performance.

The present study introduces an automatic robot work object calibration model and proposes a method that combines a 2D image sensor with the visual servo technique to establish a calibration system. The calibration process is as follows:

1. The calibration system is installed on the end effector of the robotic arm, and the coordinate transformation relation between the robotic arm and image sensor is obtained using the image data of the three axes in the robotic arm reference coordinate frame.
2. An image approximation method is employed to obtain 3D Coordinates on the 2D images, and the robotic arm is rotated around an arbitrary axis of the tool object coordinates at a fixed angle to generate a virtual image sensor, virtual TCP, and hybrid vision data.
3. A motion vector is generated using the 2D hybrid vision data in order, and the virtual TCP is made to coincide with the feature point on the work object to collect the data of the calibration reference point.
4. The data of the WOCF are obtained using that of the reference point.

Using the proposed method, work object calibration can be completed automatically and simply. The relation between the sensor and robotic arm reference coordinate frames does not need to be acquired in advance; instead, calibration can be completed by connecting through USB or TCP/IP to a computer and following the preceding procedures. Generally, obtaining additional reference points results in error averaging, improving the calibration result.

CONFLICT OF INTEREST

The authors declare no conflict of interest.

AUTHOR CONTRIBUTIONS

C. K. Huang and C. Y. Yang conceived of the presented idea. C. K. Huang developed the theory and performed the computations. B. C. Hsu and Yi-Ying Lin verified the analytical methods. C. H. Chen encouraged C. Y. Yang to investigate the work object calibration method and supervised the findings of this work. All authors discussed the results and contributed to the final manuscript.

ACKNOWLEDGMENT

This research is funded by the Technology Development Program of Ministry of Economic Affairs (project number: K368C22300) and supported by the private capital of Industrial Technology Research Institute, which guaranteed the success of this research. Therefore, we would like to show our gratitude to the two institutes.

REFERENCES

[1] International Federation of Robotics, World Robotics Report 2019, 2019.

[2] J. J. Tan, H. Gu, J. S. Li, Y. Xu, S. J. Cheng, L. Mao, “Method for work piece calibration and robot system using the same,” U. S. Patent 20190232499, Apr. 09, 2019.

[3] T. Y. SvenssonMagnus, K. G. Haage, “Method and a system for facilitating calibration of an off-line programmed robot cell,” U. S. Patent 7945349, June 09, 2008.

[4] P. Fixell, “Method and system for determining the relation between a robot coordinate system and a local coordinate system located in the working range of the robot,” U. S. Patent 7979159, Apr. 30, 2008.

[5] P. D. Smet, “Robot-cell calibration,” U. S. Patent 2009157226, Nov. 19, 2004.

[6] S. H. Wu, Y. Q. Sun, S. J. Ning, Q. Tang, Z. X. Gan, W. Wei, “Method for calibrating workpieces coordinate system,” C. N. Patent 100489448, June 30, 2006.

[7] P. Liu, H. G. Liu, S. H. Wu, Y. Q. Sun, Q. Tang, Z. X. Gan, “Workpieces reference frame marking method based on relative measurement,” C. N. Patent 100489449, June 30, 2006.